LAWRENCE
LIVERMORE
NATIONAL
LABORATORY

UCRL-PROC-212534

Integrated Experimental and Modeling Studies to Predict the Impact Response of Explosives and Propellants

J.L. Maienschein, A.L. Nichols III, J.E. Reaugh, M.E. McClelland, P.C. Hsu

May 25, 2005

JANNAF 22nd Propulsion Systems Hazards Subcommittee Meeting
Charleston, SC, United States
June 13, 2005 through June 17, 2005

INTEGRATED EXPERIMENTAL AND MODELING STUDIES TO PREDICT THE IMPACT RESPONSE OF EXPLOSIVES AND PROPELLANTS

Jon L. Maienschein, Albert L. Nichols III, John E. Reaugh,
Matthew E. McClelland, Peter C. Hsu

Lawrence Livermore National Laboratory
P.O. Box 808, L-282
Livermore, CA 94551 USA

ABSTRACT

Understanding and predicting the impact response of explosives and propellants remains a challenging area in the energetic materials field. Efforts are underway at LLNL (and other laboratories) to apply modern diagnostic tools and computational analysis to move beyond the current level of imprecise approximations towards a predictive approach more closely based on fundamental understanding of the relevant mechanisms. In this paper we will discuss a set of underlying mechanisms that govern the impact response of explosives and propellants: (a) mechanical insult (impact) leading to material damage and/or direct ignition; (b) ignition leading to flame spreading; ((c) combustion being driven by flame spreading, perhaps in damaged materials; (d) combustion causing further material damage; (e) combustion leading to pressure build-up or relief; (f) pressure changes driving the rates of combustion and flame spread; (g) pressure build-up leading to structural response and damage, which causes many of the physical hazards. We will briefly discuss our approach to modeling these mechanistic steps using ALE 3D, the LLNL hydrodynamic code with fully coupled chemistry, heat flow, mass transfer, and slow mechanical motion as well as hydrodynamic processes. We will identify the necessary material properties needed for our models, and will discuss our experimental efforts to characterize these properties and the overall mechanistic steps, in order to develop and parameterize the models in ALE 3D and to develop a qualitative understanding of impact response.

INTRODUCTION

The response of energetic materials when subject to impact stimuli is a key element in determining the hazards presented by systems containing energetic materials. The wide range of energetic materials and the many different configurations in which they are used makes it difficult to fully assess the hazards through simple experimentation. For example, the behavior will often be quite different for impact with objects of different shapes and velocities, and for the same energetic material in systems with different impact attenuators.

Our goal is to develop a predictive capability for hazards response of energetic material systems based on: A) identification of the relevant processes in chemical reaction, heat flow, and material motion that govern the hazards response; B) characterization of the relevant properties of the energetic material; C) application of these data to develop predictive mathematical models of the material behavior; and D) incorporation of the models into modern high-fidelity computer codes to allow predictive simulation of the behavior of actual systems containing these materials. In this paper we discuss our overall approach, with a primary focus on the first two elements. Our efforts are focused on non-shock impact response of energetic materials; shock response has been relatively-well studied in the past and is not included here.

In this paper we outline the underlying chemical and physical processes that control hazards response of energetic materials. We will then describe our experimental activities to characterize energetic materials behavior in these processes, including thermal ignition, thermal and mechanical properties, and fracture/ fragmentation behavior. We will present our current results on deflagration reaction rates and change in material properties through damage. Within our overall framework of understanding, our experimental results provide a means to qualitatively assess the nature of expected hazards response based on comparison of properties with those of other materials for which a significant level of experience has been developed. This is useful until such time as the predictive models become mature and productive. We will discuss insights we have developed along these lines.

MECHANISMS RELEVANT TO HAZARDS RESPONSE

At the most basic level, hazards response is driven by chemical reactions of the energetic material, which are initiated by high temperature. High pressure generally accelerates reactions, but most often does not initiate them, as shown by the fact that energetic materials are routinely pressurized to 200 MPa in pressing operations and have been studied at pressures in excess of 10 GPa in a diamond anvil cell.[1] Therefore, critical factors in the onset of reaction are those that generate, concentrate, and dissipate heat. For materials at high temperature, heat is generated by exothermic decomposition and dissipated by thermal conduction, and the balance between these determines when an explosion is ignited. For materials under impact, heat may be generated through mechanisms such as crushing or shearing of materials or frictional work along material boundaries, and may be concentrated through the formation of hot spots as in energetic materials under shock. Once reaction is underway, the speed with which the reaction propagates through the materials (and hence the rate at which energy is released) determines the violence of reaction. The speed is determined by the chemical reactions themselves, the physical condition of the energetic material (e.g. increased surface area leading to faster reaction), and the physical nature of the complete system (e.g. high confinement leading to high pressures and faster reactions). The nature and extent of damage that the

---

This work was performed under the auspices of the U. S. Department of Energy by the University of California, Lawrence Livermore National Laboratory under Contract No. W-7405-Eng-48.

energetic material has sustained can play a determining role in the violence of the ensuing reaction. The interactions among these mechanisms are illustrated in Figure 1.

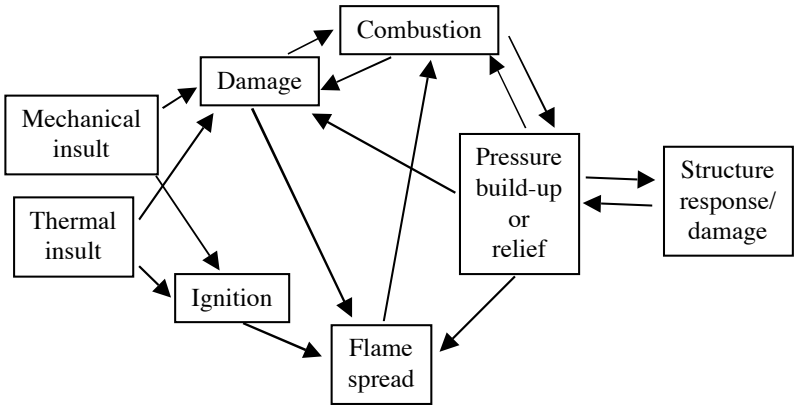

Figure 1. Physical and chemical steps in hazards response of energetic materials, and their interactions.

The reactions represented in Figure 1 are initiated either with a mechanical or thermal stimulus, as shown at the left side of the figure. Although the scope of this paper is impact response, Figure 1 illustrates the commonality between impact and thermal response of explosives - once beyond the specific stimulus, the same underlying processes govern the response to both mechanical and thermal stimuli. This is because the chemical reactions leading to an energetic response are initiated by high temperature, as explained above. This is a very important observation, because it allows us to apply the considerable body of work on thermal explosion to the associated problem of mechanical impact.

A brief description of each arrow in Figure 1 will lay the foundation for our experimental activities, which are focused on identifying and characterizing the material properties and reactions that control these steps. While thermal *ignition* is caused by a high temperature *thermal stimulus* in a fairly straightforward way, a non-shock *mechanical stimulus* may create high localized temperatures leading again to thermal *ignition* via several mechanisms such as friction between the energetic material and container, shear within the energetic material, fracture and intergranular friction in the energetic material, or compaction with void collapse and heating. The challenge is to relate heat localization to mechanical properties in simulations, and the mechanical behavior of the energetic material before, during, and after material failure is key. Material *damage* may be caused by mechanical or thermal stimulus, and will be different in nature for these two cases. In the event of a slowly-developing thermal or mechanical insult, the damaged state of the energetic material will change throughout the duration of the event and the material damage is an integral part of the overall response. In most cases the damaged material is expected to be more reactive. Damage may be characterized by surface area, porosity, and permeability to gas flow. The *flame spread* over available surfaces and into cracks is much faster than propagation of a flame into the interior of the material, and will be strongly affected by material damage – greater damage indicates greater porosity and permeability and hence greater opportunity for flames to spread over more surface area. The ignited surface will undergo *combustion* at a rate characteristic of the material and its environment, and may lead to more material damage. The combustion releases hot gaseous products which cause *pressure build-up* in the system surrounding the energetic material, accelerating the flame spreading and combustion reactions until the system fails mechanically with *relief* of the pressure or until the system proceeds to a runaway explosion with violent *structure response and damage*. A major goal of this work is the quantitative prediction of the violence of the ultimate structural response under non-shock mechanical insult. This offers several technical challenges, including developing appropriate measures of violence. An additional challenge is that some energetic materials are known to exhibit a broad range of reaction violence to nominally the same stimulus. (Composition B is one such material that exhibits an occasional violent response.)

CHARACTERIZATION OF ENERGETIC MATERIALS BEHAVIOR

In the following section we describe our experimental characterization of energetic materials, designed to address steps in the overall reaction mechanism in Figure 1. We present results on a family of RDX-based energetic materials to illustrate our approach: Composition B (~64% RDX, ~36% TNT), Composition C-4 (91% RDX, 9% oil), and PBXN-109 (64% RDX, 20% Al, 16% HTPB binder).

THERMAL IGNITION

We measure thermal ignition kinetics using the One-Dimensional Time to Explosion (ODTX) test, as described by McGuire. [2] In this test, a spherical sample 12.7 mm in diameter is held with a high-temperature isothermal boundary temperature and the time to explosion is measured; the results over a wide range of temperatures provide the kinetic information needed to develop a multi-step thermal ignition model. The experiments are conducted either with mechanical and pressure confinement of 150 MPa or with only mechanical confinement (gases are allowed to leak out). Samples are prepared by pressing (RDX, TNT, Composition B) or hand forming (PBXN-109, C-4). Results are shown in Figure 2, along with data for pure RDX and pure TNT for comparison.

An inspection of the data shows several features. In general, the ignition times at low temperatures are fairly close for all materials. At high temperatures there is a considerable spread in ignition times, with C-4 and PBXN-109 having longer ignition times. In addition, the ignition times for PBXN-109 are not dependent on the confinement of gas. The convergence of behavior at low temperatures occurs because, at these long ignition times, the samples have more or less reached thermal equilibrium, the importance of thermal transport is reduced, and ignition is governed by the reaction kinetics of RDX. At high temperatures thermal transport becomes important, in that a material with high thermal conductivity (such as aluminum-loaded PBXN-109) dissipates the exothermic heat of reaction and therefore requires a higher ignition temperature than a material with low thermal conductivity (such as RDX).

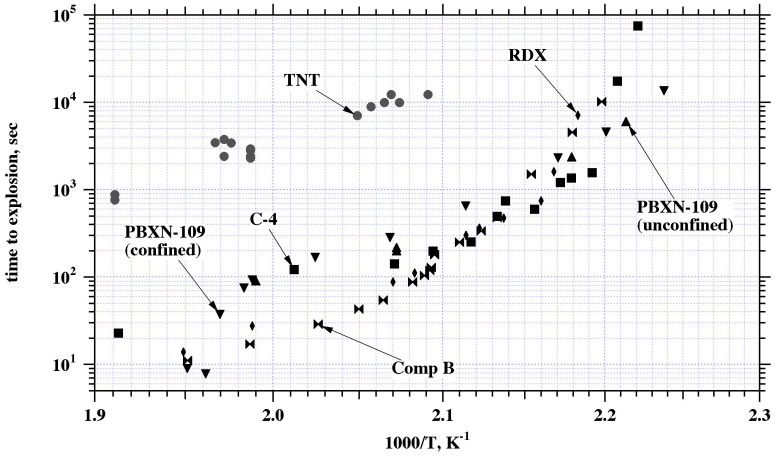

Figure 2. ODTX data for the family of RDX-based energetic materials. TNT is included as the "binder" in Comp B.

We use the data shown in Figure 2 to create thermal ignition models for each energetic material. The methodology is described by McClelland.[3,4] The models are directly applicable to the ignition step in Figure 1, and qualitative observations as described above provide immediate understanding of the relative behavior of materials.

MECHANICAL IGNITION

Ignition from mechanical deformation is not well understood. As mentioned above, there are several possible mechanisms, including friction between the energetic material and container, shear within the energetic material, fracture and intergranular friction in the energetic material, and compaction with void collapse and heating. Most current experimental activities are aimed at identifying the relevant mechanism, not parameterizing a model, since the mechanisms are so poorly known.

One approach is the recent measurement of friction of energetic materials with different materials including itself, reported by Hoffman.[5] This work was done with an 85% HMX / 15% Viton energetic material (LX-04) and aluminum, steel, and PTFE. The coefficients of friction were reported as a function of temperature, and decreased with increasing temperature, as expected, except with aluminum; in that case it was postulated that the Viton fluoroelastomer abraded the protective oxide coating from the aluminum and reacted with the exposed aluminum. This work was done to help parameterize a frictional work model for mechanically-induced ignition, as reported by Chidester.[6]

THERMAL AND MECHANICAL PROPERTIES

Thermal properties of particular importance are specific heat, thermal conductivity, and coefficient of thermal expansion. Most often we use room temperature values of these properties with pristine materials, but to improve the fidelity of simulations we are measuring these parameters as a function of material temperature and damage state. Specific heat and thermal expansion measurements for pristine PBXN-109 were reported by McClelland,[3] and results are shown in Figure 3. The specific heat increases by 25% from 40°C to 140°C, showing the importance of accurately measuring such properties over a range of conditions. We are just now obtaining the capability to measure thermal conductivity of energetic materials over a wide range of temperatures. Similar measurements have been or are being made on other materials of interest. Characterization of damaged materials is discussed below.

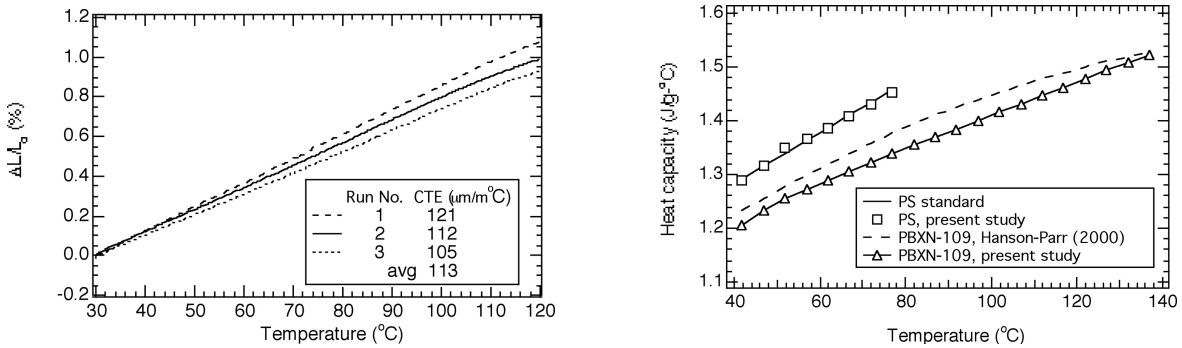

Figure 3. Thermal expansion (left) and specific heat (right) measurements for PBXN-109 at temperatures up to 130°C. Details of the methods are given by McClelland.[3]

The effects of a non-shock mechanical deformation are critical in determining ignition from mechanical stimuli. As described above, the challenge is to relate heat localization to mechanical properties in simulations, and the mechanical behavior of the energetic material before, during, and after material failure is key. Mechanical properties of importance include shear modulus, bulk modulus, elastic modulus, and Poisson's ratio, again over a wide range of temperatures and material damage. Measurement of the shear and bulk moduli, and estimation of the elastic modulus and Poisson's ratio, were reported by McClelland. [3] Results for the shear and bulk moduli are shown in

Figure 4. As expected, the shear moduli decrease with increasing temperature, although the effect is low. We do not have compressive strength and bulk moduli as a function of temperature.

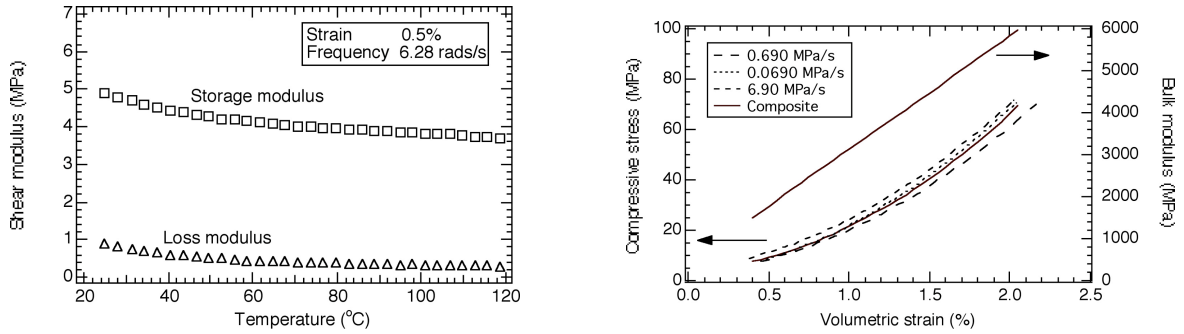

Figure 4. Shear moduli for PBXN-109 as a function of temperature (left), and compressive stress and bulk modulus for PBXN-109 at 22°C. The shear moduli were measured at 1 cycle/sec and 0.5% strain. Details are given by McClelland. [3]

The thermal and mechanical data for PBXN-109 represent the type of data needed to develop models for the mechanical stimulus and thermal stimulus steps in Figure 1. These models will also be important in other steps in the overall mechanism, such as the effect of mechanical properties on the behavior of the material during dynamic pressurization such as explosion.

FRACTURE / FRAGMENTATION BEHAVIOR

The fracture behavior of energetic materials under mechanical stimulus is a critical element in the understanding of response to mechanical impact. During mechanical deformation and fracture the energetic material components may undergo frictional heating from interactions between fragments. Once ignition has occurred, fragmentation leads to greatly-increased surface area in the energetic material and hence a much higher effective burn rate in terms of energy release and gas production. The extent of surface area increase from fragmentation is therefore very important.

Our current model for energetic material fragmentation is based on the simple hypothesis that the local fragment surface area depends on strain and on strain rate. As a result, our model allows fragmentation to occur even though gas pressure from decomposition products keeps the pressure compressive. With this model, we have captured the particle size distribution and its dependence on impact velocity that results from the shotgun test of propellants with the same binder as PBXN-109 (AP/Al/HTPB propellants). The linear strain-rate dependence of our model predicts that large pieces of energetic material will produce the same number of fragments as small pieces, provided that the impact velocity is the same. This result is in qualitative accord with observation, but requires detailed analysis of the fragments resulting from large scale impacts to be proven quantitatively accurate; this latter step is made more difficult by the fact that larger pieces tend to react in impact tests.

The shotgun test test comprises a two-step procedure for measuring the damage to rocket propellants that results from impact. In one version of this test, [7] 8-gram samples of energetic material are fired from a 12-gauge shotgun at a thick steel plate. The impact debris are recovered and burned in a closed combustion bomb, with the pressure recorded during the burn. The rate of pressurization of damaged energetic material depends on the laminar burn rate, which is a property of the energetic material, and on the surface area, which is a measure of damage. By measuring the burning rate of undamaged propellant, the surface area of damaged propellant can be determined. [7] Impacted samples using a representative propellant are shown in Figure 5.

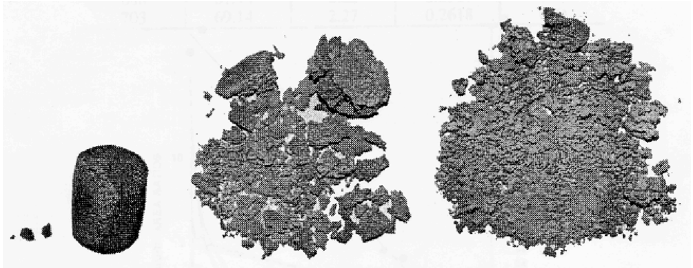

Figure 5. Results of shotgun tests on a representative HTPB propellant with impact velocity 92 m/s (left), 151 m/s (center), and 214 m/s (right). Figure from Atwood. [7]

Our model for fragmentation is consistent with the ideas of comminution. [8] From that perspective, materials are ground finer by the application of energy, transforming mechanical work into surface energy. The basic idea, then, is that the local strain energy is used to produce the local fragmentation - the higher the strain energy, the smaller the fragments. Following this idea, we model the surface to volume ratio of a material under a specific stress state as:

$$\left(\frac{S}{V}\right)_0 = A(\varepsilon - \varepsilon_0)\langle\dot{\varepsilon}\rangle \qquad \text{Eq. (1)}$$

where the subscript 0 indicates that this is the initial *S/V* ratio before burning starts. The equivalent plastic strain, e, must exceed a threshold value, e_0, which corresponds to the strain where little damage occurs. (See Figure 5) The S/V ratio is also proportional to the average plastic strain rate. This is the method we chose to describe the effects of scale, wherein the number of fragments produced in two geometrically scaled impacts will be the same. The result that impacts of big objects make big pieces is qualitatively supported by observation. We chose a specific form for the average strain rate,

$$\langle \dot{\varepsilon} \rangle = \frac{\int_0^t \dot{\varepsilon}(t')\left[\dot{\varepsilon}(t')dt'\right]}{\int_0^t \dot{\varepsilon}(t')dt'} \qquad \text{Eq. (2)}$$

which we call the strain-averaged strain rate. We separate the numerator integrand, which is the square of the strain rate, to highlight the structure. The bracketed factor is just the differential of the strain. The reason for our choice of weighting is that the value of our average strain rate will stay constant after a transient impact. If the strain doesn't increase, the average strain rate won't change. With a simple time-averaged value, the average strain rate will decrease after the impact, depending on how long one waits. Without averaging of some kind, the finite-difference analog of the strain rate will be noisy, and have artificially high value.

To fit this model to shotgun test results, we calculated the strain history in the samples during impact and compared this with the pressure data from the closed bomb burner. From this we calculated parameters $e_0 = 0.1$, A = 700 msec/mm for a range of HTPB propellants under study. The fit was reasonably good; the model predicted the end piece of the sample impacted at intermediate velocity would remain intact, as in fact it did (Fig. 5).

This model is being extended to a wider range of materials, and its applicability for these remains to be demonstrated. Nonetheless it is a practical model to estimate the increase in surface area of an energetic material sample under mechanical deformation.

DEFLAGRATION BEHAVIOR

Deflagration behavior of the energetic material (combustion in Figure 1) determines the rate of energy release and hence is a key factor in overall reaction violence. We measured the deflagration rate of PBXN-109, Composition B and Composition C-4 at high pressures (10-700 MPa) and temperatures (20 – 180°C), using the LLNL high pressure strand burner. This instrument, shown schematically in Figure 6, combines the features of a traditional closed-bomb burner with those of a traditional strand burner. The LLNL high-pressure strand burner contains a burning sample in a small volume, high-pressure chamber. We measure temporal pressure data and burn front time-of-arrival data to get the laminar burn rate for a range of pressures in one experiment. We use a pressure transducer and a load cell to measure the temporal pressure in the bomb, and detect the arrival of the burn front by the burning-through of thin wires embedded in the sample. High speed digital scopes capture the data for subsequent analysis. In contrast, with a standard closed-bomb burner, pressure in the combustion chamber is the only measurement; calculation of the burn rate requires accurate knowledge of the equation of state of the product gases and accurate treatment of heat losses. There is no measure of the surface regression rate to check combustion uniformity, so data from samples that burn erratically are particularly hard to interpret. The standard strand burner provides direct measurement of the surface regression rate in a large volume at constant pressure, giving only one pressure/rate data point in each experiment; furthermore, the large volume required for isobaric operation means that operation at high pressures is generally not practical. Further details on this apparatus are given by Maienschein. [9,10]

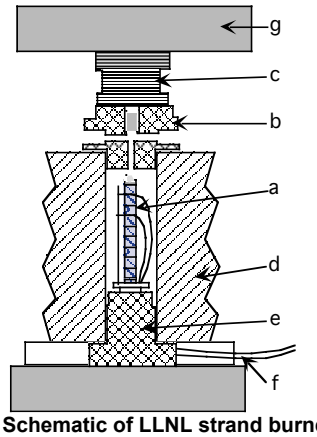

a - nine-segment burn sample, with burn wires between segments (only two wires shown for clarity) and ignitor on top;
b - top plug with inlet and outlet ports and pressure transducer in center;
c - load cell;
d - pressure vessel;
e - bottom plug with wire feedthroughs;
f - signal wires to electronics;
g - load frame (top and bottom)

Figure 6. Schematic of LLNL strand burner

The deflagration behavior of the three materials at room temperature is shown in Figure 7-9. Results at high temperature are reported by Maienschein. [10]The deflagration behavior of PBXN-109 in Figure 7 is remarkably stable over the entire pressure range, with data showing smooth and consistent increases with pressure within each run and from run to run. Also shown in Figure 7 are data at the lower end of our pressure range measured at NAWC. [11] The LLNL and NAWC results show excellent agreement. Our burn rate data show a slope change around 135 MPa. Power-law parameters and line fits are shown for the low-pressure and high-pressure regions. The pressure exponent decreases significantly at pressures above 135 MPa from greater than 1 (1.32) to less than 1 (0.85).

Composition B exhibited deflagration behavior unlike that of other materials that we have tested. In virtually every case (Figure 8), the first few pellets burned relatively slowly and with apparent uniformity, but later pellets burned very rapidly and erratically. The first few pellets provide a measurement of the uniform deflagration rate of Composition B before it undergoes the transition to rapid deflagration. The fit to the lower edge of the data set, representing the burning of the first few pellets, shows a second-order pressure dependence, very high compared with all other materials we have tested. The high pressure dependence of Composition B deflagration has been previously

observed. Birk reported results from interrupted burning tests at pressures up to 70 MPa, and found an overall pressure dependence of 1.7. [12] Later work by the same group showed the pressure exponent ranging from 1.5 to 1.7 in measurements with a strand burner at 2-10 MPa and with a closed bomb at 10-100 MPa. [13] We interpret the onset of rapid burning as the onset of deconsolidation of the sample – the sample loses mechanical integrity and develops high surface area, leading to rapid deflagration. The first few pellets burn with apparent uniformity and the following pellets burn rapidly, regardless of the initial pressure. Therefore the deconsolidation process in Composition B seems to be time dependent instead of pressure dependent as in HMX-based energetic materials. [9] This may be a result of dynamic melting of the TNT during the deflagration process in the high-temperature environment of the pressure vessel.

Composition C-4 exhibits deflagration behavior (Figure 9) between that of PBXN-109 and Composition B. At low pressures the deflagration is uniform, but at pressures above 70 MPa the deflagration rate starts to rapidly climb, indicative of deconsolidation.

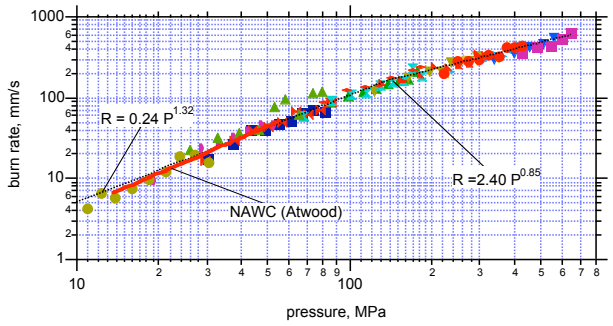

Figure 7. Deflagration rate data for pristine PBXN-109. Solid symbols are LLNL measurements. Each set of symbols represents data from one experiment. A fit to data from NAWC (Alice Atwood) [11] is shown by the solid line. Power-law fits to low and high pressure regions are shown by the dotted lines.

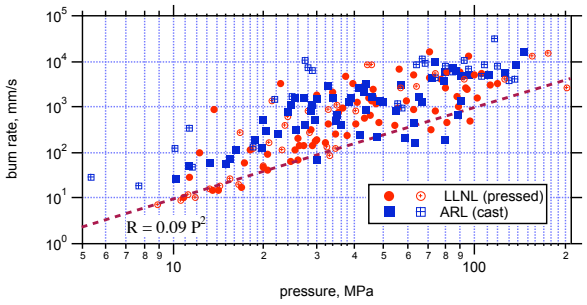

Figure 8. Deflagration rate data for Composition B (pressed and cast samples). Dotted line shows fit to the lower edge of the data set, and parameters for the fit are also listed. Hollow and solid symbols represent different sample assembly methods – all samples showed the same behavior.

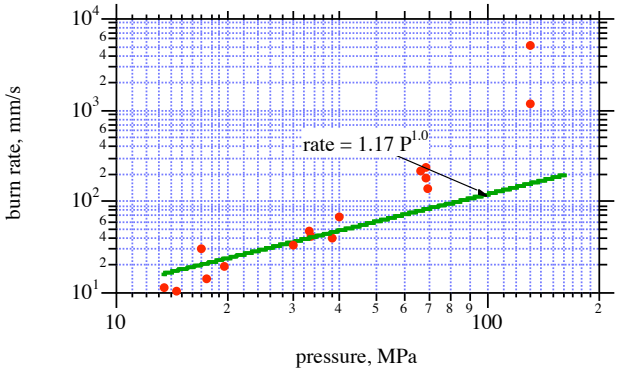

Figure 9. Deflagration rate data for Composition C-4. The symbols represent deflagration rates measured for specific sections of the sample. The solid line is a fit to the low-pressure data which show uniform deflagration.

In comparing these three formulations, we see very similar deflagration with PBXN-109 and Composition C-4 before the onset of deconsolidation with approximately 1st-order pressure dependence; however, PBXN-109 with its HTPB binder maintains mechanical integrity and does not undergo deconsolidative burning at any pressures, while Composition C-4 with its oil binder has low mechanical strength and does physically fail. Composition B has a very different behavior, with a 2nd-order pressure dependence before deconsolidation.

MATERIAL DAMAGE

As described above, material damage may be caused by mechanical or thermal stimulus, and will be different in nature for these two cases. A slowly-developing (minutes to hours) thermal stimulus may lead to an evolving damage state as the event proceeds, and the changing material damage is an integral part of the overall response. Mechanical damage will occur more rapidly (microseconds to seconds). In most cases the damaged material is expected to be more reactive.

In determining the definition and diagnostics for material damage, we consider the effect of damage on the response processes shown in Figure 1. The production of porosity and increase in permeability (connected pores) increases the surface area for flame spread and combustion, so porosity, permeability, and surface area are key damage parameters. Characterization of the deflagration behavior of damaged material represents an integration of the above factors and can provide an independent way to represent the effects of damage. Of perhaps lower importance are the changes in thermal and mechanical properties and density.

We are measuring permeability and surface area for thermally and mechanically-damaged energetic materials. We use a commercial permeameter (Porous Materials Inc, Ithaca NY) to measure gas permeation, and a standard BET apparatus to measure surface area. In preliminary results, we found that an 85% HMX / 15% Viton energetic material (LX-04) showed no permeability change when heated

to 140°C (permeability < $1x10^{-20}$ m^2, limit of detectability), and showed a permeability of $2x10^{-18}$ m^2 when heated to 190°C. This is consistent with observations made with PBX9501 by Parker. [14] In tests with a mock energetic material of varying densities and degrees of damage, we found that the permeability was well correlated with $e^3/(1-e)^2$, where e is the porosity. This is the functionality predicted by the Blake-Kozeny equation[15] for gas flow through a porous media, and represents a promising candidate for thermal damage simulations involving evolution of permeability. [16] Hsu also reports on the change in density and sound speed in pristine and damaged mock energetic material.

Work in characterizing damaged energetic materials is still immature, but clearly represents an important component of the overall hazards response understanding.

OTHER AREAS

Referring to Figure 1, we identify flame spreading as an area where knowledge is lacking and there is not significant research underway. Pressure build-up or relief depends on production of gas and heat from the combustion process and change in system volume from structural response. Therefore, understanding the structural response, which generally depends on the behavior of non-energetic structural elements, is also key to the problem.

INTEGRATED TEST - SCALED THERMAL EXPLOSION EXPERIMENT

We developed the Scaled Thermal Explosion Experiment to experimentally explore the integration of all the response processes in thermal explosion. Because of the strong connections between thermal response and mechanical impact, test results also are relevant to impact response, and the test is therefore briefly discussed here. We developed the Scaled Thermal Explosion Experiment with the following goals in mind: uniform heating for well-defined boundary conditions; well-defined physical confinement; pre-determined reaction location away from end effects; a range of physical scales; quantitative measurements of reaction violence; and a design to allow accurate simulations of the system while avoiding physical features that are difficult to model. To this end, we devised a cylindrical test, shown in Figure 10, where the reaction initiates in the axially central region of the cylinder (radial location depends on heating rate). Confinement is determined by a steel wall and thick end caps, with rupture pressures of 50, 100, or 200 MPa. Most experiments have been conducted with sample diameter of 51 mm and length of 203 mm. The vessel is externally heated until it explodes. Diagnostics include thermocouples and thermisters at many locations, strain gauges, an internal pressure gauge on some experiments, and measurement of the wall velocity during the explosion using micropower impulse radar. Further details are given by Wardell. [17]

Several STEX tests have been run with the family of RDX-based energetic materials. The results are shown in Table 1. The relation of wall velocity to energy release as a percent of detonation energy is discussed by Wardell. [17] We assess reaction violence from the number and size of wall fragments(many small fragments indicates high violence, few large fragments indicates low violence), the wall velocity, and the radial strain rate. Composition B showed uniformly high reaction violence - only at low confinement and a fast heating rate did it give a low degree of violence. PBXN-109, on the other hand, showed very mild reaction violence even with a high degree of confinement and slow heating. Composition C-4 was quite violent, particularly considering the low confinement with which it was tested.

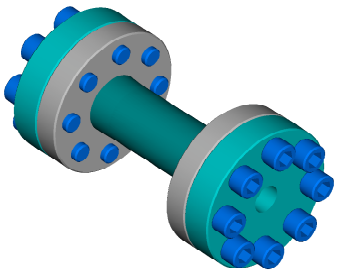

Figure 10. Designer's rendition of the 51 mm STEX vessel. Note the vessel tube, brazed flanges, thick end caps and large bolts.

Table 1. Summary of scaled thermal explosion experiments results with RDX-based energetic materials. For all: 51 mm diameter, 203 mm length; ramp rate above 130°C is shown. Onset temperature is highest reading on vessel exterior at time of runaway reaction. All vessels were sealed, with no visual or audible evidence of venting. Violence is indicated by fragment distribution, by peak wall velocities measured by radar, by calculation of percent of detonation energy, and by peak wall strain rate.

Test #	Confinement, MPa	Ramp rate, °C/hr	Onset temp. °C	Frag-ments*	Wall velocity† (3 channels), m/s	"Average" wall velocity, m/s	% of detonation energy	Log (peak wall radial strain rate, s^{-1})
Composition B								
12	200	1.0	159	37S	2100, 2000, x	2000	100	2.0
13	200	1.0	160	52S	2000, 2800, 1000	1300	45	-
17	200	2.0	164	48S	x, 1800, 600	700	13	2.5
18	200	3.0	166	48S	1100, 900, x	880	20	1.7
19	100	1.0	164	22S	2500, 2500, x	2500	100	2.7
20	100	3.0	169	1S**	200, x, x	200	1	1.7
PBXN-109								
36	200	1.0	152	3L	250, 450, 180	200	1	2.6
Composition C-4								
40	50	1.0	169	24S	2500, 2300, 2200	2200	50	3.0

* L: large frags several cm largest dimension; S: small frags ~ 1-2 cm.;
** vessel wall was largely intact, but greatly deformed. One fragment was ejected.
† in some cases, radar channel did not report. Missing data are shown as x.

INTEGRATED TEST – STEVEN IMPACT TEST

An integrated test for mechanical response of energetic materials is the Steven Impact Test, as described by Chidester. [6] Tests are underway with different types of explosives, and the results will be reported at future meetings.

SIMULATION OF MECHANISTIC STEPS OF IMPACT RESPONSE USING ALE3D

The ALE3D code is a coupled thermal-hydro-chemical code that has been under development at LLNL for several years.[18, 19] It includes fully coupled chemistry, heat flow, mass transfer, and slow mechanical motion as well as hydrodynamic processes. The current version of ALE3D began as a 3D ALE hydrocode to which has been added several capabilities. These include implicit thermal transport, thermally driven reactions, models for both the thermal and mechanical properties of chemical mixtures, second order species advection, and implicit hydrodynamics. Features include automated transition between implicit and explicit calculational schemes, propagation of deflagration reactions using a level-set model, a multi-material deflagration model, thermal transport through mixed elements, and slide surfaces. More details are given by Yoh et al. [18, 19] For impact response, models of the material properties described above have been or are being developed. The integrated nature of ALE3D provides a natural framework to take advantage of the similarity of response mechanisms between thermal and impact response.

QUALITATIVE INSIGHTS FROM EXPERIMENTAL DATA

We can draw some qualitative insights on impact response from the material characterization data above. The ODTX data suggest that the thermal ignition of the RDX-based energetic materials should be similar at low temperatures, and indeed the ignition temperatures for the three materials in the STEX data were fairly consistent at 152 – 169°C. Given the similarity of ignition behavior, the conversion of mechanical deformation to regions of high temperature sufficient to ignite reaction will therefore control the impact response. Materials that dissipate mechanical energy uniformly (e.g. rubbery materials such as PBXN-109 or malleable materials such as Composition C-4) are therefore expected to be much less sensitive to mechanical impact than materials that are brittle and/or easily fragmented such as Composition B. The degree of violence following the onset of reaction from impact is expected to be consistent with the deflagration behavior. The pressure dependence of the deflagration rate is significant - for materials with a low pressure dependence of high-pressure deflagration, such as PBXN-109 and Composition C-4 (n~1), the reaction rate is accelerated relatively slowly. In contrast, for a material with a high pressure dependence for deflagration, such as Composition B (n~2), the high-pressure deflagration is accelerated at a very high rate, leading to very violent explosions. In addition, the deconsolidation leading to high deflagration rates with Compositions B and C-4 drive the violence even higher. For Composition C-4, at least, this latter effect is most important since its pressure exponent is ~ 1. O

In summary, we expect that PBXN-109 and Composition C-4 require a stronger mechanical insult to initiate a reaction than Composition B. When impacted sufficiently strongly to initiate reaction, we expect Composition B to give the most violent reactions (high pressure dependence of deflagration and deconsolidative behavior), with Composition C-4 giving more violent responses than PBXN-109 (deconsolidate deflagration in the former). Impact experiments (Steven Tests) are underway or planned to test these predictions.

SUMMARY

We have presented an integrated mechanism for hazards response of energetic materials, which provides a conceptual framework to define material characterization and response studies. We illustrate the application of this approach by presenting data for a series of RDX-based energetic materials in impact response and related thermal explosion experiments. Consideration of the characterization data provides qualitative insight into the hazards response behavior of the materials. Use of the characterization data to develop material models that are incorporated into a suitable simulation code will ultimately provide a predictive capability for a wide range of scenarios – this is our long-term objective in the area of hazards response of energetic materials.

We note that the studies reference herein represent an incomplete set of the current research in this field – the primary purpose of this article is to desribe the approach being undertaken at Lawrence Livermore National Laboratory as well as at other institutions.

ACKNOWLEDGEMENTS

We would like to acknowledge the contributions of our colleagues at US DOE and DoD laboratories, as well as colleagues in Europe, with whom we have had many discussions over the last several years. We acknowledge financial support from the LLNL HE Response Program and the Joint DoD/DOE Munitions Technology Development Program.

REFERENCES

1. M.F. Foltz and J.L. Maienschein, “Ammonium perchlorate phase transitions to 26 GPa and 700 K in a diamond anvil cell,” *Materials Letters*, **24**, 407 (1995).
2. R.R. McGuire and C.M. Tarver, “Chemical Decomposition Models for the Thermal Explosion of Confined HMX, TATB, RDX,and TNT Explosives,” in *Proceedings of Seventh Symposium (International) on Detonation*, Annapolis, MD, Naval Surface Weapons Center, NSWC MP 82-334, p. 56 (1981).
3. M.A. McClelland, T.D. Tran, B.J. Cunningham, R.K. Weese and J.L. Maienschein, “Cookoff Response of PBXN-109: Material Characterization and ALE3D Model,” in *Proceedings of JANNAF 19th Propulsion Systems Hazards Subcommittee Meeting*, Monterey, CA, CPIA, Publication 704 Vol I, p. 191 (2000).
4. M.A. McClelland, J.L. Maienschein, A.L. Nichols, J.F. Wardell, A.I. Atwood and P.O. Curran, “ALE3D Model Predictions and Materials Characterization for the Cookoff Response of PBXN-109,” in *Proceedings of JANNAF 38th Combustion and 20th Propulsion Systems Hazards Subcommittee Meetings*, Destin, FL, CPIA, Publication JSC CD-14, (2002).
5. D.M. Hoffman and J.B. Chandler, “Aspects of the Tribology of the Plastic Bonded Explosive LX-04,” *Propellants, Explosives, Pyrotechnics*, **29**, 368 (2004).
6. S.K. Chidester, L.G. Green and C.G. Lee, “A frictional work predictive method for the initiation of solid high explosives from low-pressure impact,” in *Proceedings of 10th International Detonation Symposium*, Boston, MA, Office of Naval Research, ONR 33395-12, p. 786 (1993).
7. A.I. Atwood, P.O. Curran, C.F. Price, G.W. Meyers and J.R. Thompson, “Shotgun testing for the propellant sensitivity program,” Naval Air Warfare Center, Weapons Division, China Lake, CA 93555, NAWCWPNS TM 7876 (June 1995).

8. G.C. Lowrison, *Crushing and Grinding; The Size Reduction of Solid Materials*, Butterworths, London (1974).
9. J.L. Maienschein and J.B. Chandler, “Burn Rates of Pristine and Degraded Explosives at Elevated Pressures and Temperatures,” in *Proceedings of 11th International Detonation Symposium*, Snowmass, CO, Office of Naval Research, p. 872 (1998).
10. J.L. Maienschein and J.F. Wardell, “Deflagration Behavior of PBXN-109 and Composition B at High Pressures and Temperatures,” in *Proceedings of JANNAF 38th Combustion and 20th Propulsion Systems Hazards Subcommittee Meetings*, Sandestin, FL, CPIA, Publication JSC CD-14 (2002).
11. A.I. Atwood, NAWC China Lake, personal communication, 2001.
12. A. Birk, D.E. Kooker and P. Baker, “Model of Cavity Combustion Within an Energetic Solid: Application to Composition-B,” in *Proceedings of JANNAF 37th Combustion and 19th Propulsion Systems Hazards Subcommittee Meetings*, Monterey, CA, CPIA, Publication 704, Vol. II, p. 95 (2000).
13. P. Baker, Army Research Laboratory, personal communication, 2001.
14. G.R. Parker, B.W. Asay, P.M. Dickinson, B.F. Henson and L.B. Smilowitz, “Effect of thermal damage on the permeability of PBX9501,” in *Proceedings of American Physical Society Topical Group on Shock Compression of Condensed Matter - 2003*, Portland, OR, 2004, American Institute of Physics, p. 1009 (2003).
15. R.B. Bird, W.E. Stewart and E.N. Lightfoot, *Transport Phenomena*, Wiley, (1960).
16. P.C. Hsu, M. DeHaven, M.C. McClelland and J.L. Maienschein, “Thermal damage on LX-04 mock material and gas permeability assessment,” *Propellants, Explosives, Pyrotechnics*, in press, (2005).
17. J.F. Wardell and J.L. Maienschein, “The Scaled Thermal Explosion Experiment,” in *Proceedings of 12th International Detonation Symposium*, San Diego, CA, 2003, Office of Naval Research, in press (2002).
18. J. J. Yoh, M. A. McClelland, J. L. Maienschein, J. F. Wardell and C. M. Tarver, “Simulating thermal explosion of cyclotrimethylenetrinitramine-based explosive: Model comparison with experiment,” J. Appl. Phys. (2005) in press.
19. J. J. Yoh, M. A. McClelland, J. L. Maienschein and J. F. Wardell, “Towards a predictive thermal explosion model for energetic materials,” J. Comp.-Aided Matls. Design (2005) 175-179.